460
12/3/63

WAPD-276

AEC RESEARCH AND
DEVELOPMENT REPORT

Rn-220

THE EMANATION OF RADON-220 FROM SINTERED UO_2 POWDERS AND PLATES

OCTOBER 1963

CONTRACT AT-11-1-GEN-14

BETTIS ATOMIC POWER LABORATORY, PITTSBURGH, PA.,
OPERATED FOR THE U. S. ATOMIC ENERGY COMMISSION
BY WESTINGHOUSE ELECTRIC CORPORATION

DISCLAIMER

WAPD-276

UC-25: Metals, Ceramics, and Materials
TID-4500 (21st Edition)

THE EMANATION OF RADON-220 FROM SINTERED UO_2 POWDERS AND PLATES

J. C. Clayton and S. Aronson

October 1963

Contract AT-11-1-GEN-14

Price $0.75
Available from the Office of Technical Services,
Department of Commerce,
Washington 25, D. C.
Printed in U. S. A.

BETTIS ATOMIC POWER LABORATORY, PITTSBURGH, PA., OPERATED FOR THE U. S. ATOMIC ENERGY COMMISSION BY WESTINGHOUSE ELECTRIC CORPORATION

STANDARD EXTERNAL DISTRIBUTION

	No. Copies
UC-25: Metals, Ceramics, and Materials TID-4500 (21st Edition)	586

SPECIAL EXTERNAL DISTRIBUTION

Manager, Pittsburgh Naval Reactors Office, AEC	5
Director, Development Division, PNRO	3
Classification and Technical Information Officer, PNRO	1
Total	595

CONTENTS

	Page No.
I. INTRODUCTION	1
II. THEORY OF THE EMANATION PROCESS	2
III. EXPERIMENTAL	3
A. Sample Preparation and Fabrication	3
B. Characterization of Sintered Plates	3
C. Emanation Measurements	3
IV. RESULTS	4
A. Thorium X Rejection	4
B. Emanation Measurements	5
1. Sintered UO_2 Powders	5
2. Low Density UO_2 Plates	7
3. High Density UO_2 Plates	11
V. DISCUSSION	15
VI. SUMMARY AND CONCLUSIONS	17
APPENDIX A. Sample Preparation and Standardization	20
APPENDIX B. Emanation Apparatus	21
APPENDIX C. Thoron Diffusion Coefficients in Low Density UO_2 Plates	22
ACKNOWLEDGMENTS	23
REFERENCES	24

The emanation of thoron (Rn^{220}) from sintered UO_2 powders and plates was measured as a function of temperature. The uranium oxide samples were indexed with radiothorium by coprecipitation and coevaporation techniques. The emanation measurements were performed in a flow system, using an alpha scintillation detector and a helium-hydrogen carrier gas mixture. Both the radiothorium concentration (5 to 100 μc/g UO_2) and the uranium oxide density (71 to 99 percent TD) were varied. The surface areas and densities of the UO_2 plates were measured by krypton gas adsorption and liquid immersion techniques, respectively.

Assuming a diffusion mechanism, diffusion coefficients for thoron in sintered UO_2 were calculated as a function of temperature. The data were represented by an equation of the form, $D = D_0 \exp(-Q/RT)$. An apparent increase in both activation energy (Q) and D_0 with density was observed for the 1100 to 1450°C temperature range. For some samples the thoron emanating power could be measured at temperatures as low as 400°C. Log D versus 1/T plots from 400 to 1450°C gave intersecting straight lines with different activation energies. One intersection occurred near the Tammann temperature. The emanation of Rn^{220} from UO_2 apparently involves several types of diffusion processes

THE EMANATION OF RADON-220 FROM SINTERED UO_2 POWDERS AND PLATES

J. C. Clayton and S. Aronson*

I. INTRODUCTION

Isotopes of the rare gases krypton and xenon are produced within the uranium dioxide lattice by uranium fission, and evidence indicates that the release of these fission gases from UO_2 is due to diffusion through the lattice (Reference 1). Most experimental work on the diffusion of rare gases from UO_2 has involved the use of irradiated samples (Reference 1); however, the mobility of noble gases in UO_2 may also be studied by use of the natural decay products of thorium which are available commercially and which are readily incorporated in oxide structures in trace amounts. One of these compounds (Th^{228}) upon radioactive α-decay yields thoron, an isotope of radon, as a second daughter. This product is a gas, and its release from UO_2 should correlate with that of the fission gases xenon and krypton.

In this investigation sintered UO_2 powders and plates were homogeneously indexed with radiothorium, and the amount of the resulting thoron gas evolved was measured as a function of temperature. This study was undertaken in order to compare Rn^{220} release rates and diffusion coefficients with those of the fission gases. The emanation technique, besides permitting the use of unirradiated samples, allows considerable flexibility in measuring the effects of composition and structure of a ceramic body on rare gas release.

---

* Present Address: Brookhaven National Laboratory, Upton, Long Island, N.Y.

II. THEORY OF THE EMANATION PROCESS

The fraction of radioactive inert-gas atoms formed in a solid that escapes from the solid is called its emanating power. Hahn (Reference 2) was the first to correlate the emanating power and the structure of a solid. The theory and methods of measuring emanating power are well known (References 3 to 7), requiring only brief explanation in this report.

A highly emanating standard of known emanating power (barium stearate) is compared with the UO_2 sample in two ways:

(1) The relative rates of formation of inert gas in the standard and UO_2 are determined by measurement of their beta activities in sealed containers after radioactive equilibrium has been attained

(2) The relative rates of escape of the thoron gas from the standard and UO_2 are determined in a flow system:

$$\frac{E_S}{E_{UO_2}} = (A_\alpha/A_\beta)_S/(A_\alpha/A_\beta)_{UO_2} \quad (1)$$

where

A_α = the alpha activity measured in the flow system
A_β = the measured beta activity
E = the emanating power

The inert-gas atom may escape from the solid either by recoil (E_R) or by diffusion (E_D), so that the total emanating power is

$$E = E_R + E_D \quad (2)$$

Because the recoil fraction varies negligibly with temperature, the two factors can be separated by considering the room temperature emanating power as the recoil contribution and subtracting this from measurements obtained at higher temperatures to determine the diffusion contribution.

The contribution of the emanating power depends on the rate of diffusion of the emanation to the surface of the solid particle (E_D). In the case of spherical particles it is related to the inert-gas diffusion coefficient (D) by the following equation:

$$D = \lambda r^2 E_D^2/9 \quad (3)$$

where

λ = decay constant, 1.27×10^{-2} sec^{-1} for thoron
r = particle radius, cm
E_D - emanating power due to diffusion
D = inert-gas diffusion coefficient, cm^2/sec

However, high density plates, whose roughness factors (ratio of gas adsorption to geometrical surface areas) approach unity, cannot be approximated as a collection of spherical particles. In this case the inert-gas diffusion coefficient is evaluated by the equation

$$D = E_D^2 t^2 \lambda/4 \quad (4)$$

where

t = plate thickness, cm

The diffusion coefficients for thoron in sintered UO_2 powders and plates were calculated by means of the above equations.

III. EXPERIMENTAL

A. Sample Preparation and Fabrication

The Th^{228} was incorporated into the uranium oxide samples by two techniques. Tracer amounts (5 to 100 μ c/g UO_2) of radiothorium were added to uranyl nitrate solutions which were converted into UO_2 by either a coprecipitation or a coevaporation procedure. The indexed UO_2 powders were homogenized by annealing them in hydrogen for 40 hours at 1750°C. A portion of each annealed UO_2 preparation was reserved for emanation measurements. The remaining powder was ground, agglomerated with an organic binder, pressed into plates, and sintered in hydrogen at 1400 to 1750°C. The barium stearate standard was prepared by adding a hot sodium stearate solution to a barium chloride solution containing radiothorium (Reference 8). The preparation, indexing, and fabrication procedures are described in detail in Appendix A.

B. Characterization of Sintered Plates

A sintered oxide plate contains both open (connected) and closed (unconnected) pores. The total volume can be considered as the sum of the open pore volume, the closed pore volume, and the volume of the solid. The percent theoretical density (percent TD) of the UO_2 plates was determined by using a water-immersion technique. The amount of open porosity was measured by placing the wafer in a vacuum system, evacuating, and adding water. The water is assumed to enter all of the open pores. The plates are blotted dry and reweighed. This weight minus the weight in air is a measure of the open pore volume.

Since the rates of thoron emanation are proportional to the surface areas of the solids, surface area measurements by gas adsorption techniques were made on the sintered UO_2 plates. The low-temperature adsorption of krypton and ethane on low and high density compacts, respectively, was measured volumetrically (Reference 9).

The microstructure of selected sintered oxide plates was determined by using techniques described in Reference 10. Samples were mounted in a plastic medium (epoxy resin), polished with abrasives, and chemically etched (H_2SO_4-H_2O_2 solution). The polished and etched sections were viewed and photographed with bright field-reflected illumination. Because of the hazardous nature of the emitted thoron gas, all of these operations were performed remotely in a hot cell.

Thoron emanation measurements were performed on 15 separate sintered UO_2 plates whose physical properties are listed in Table 1. The beta activities, measured under standardized conditions, are included as a measure of the amount of incorporated radiothorium. The "particle" radii were calculated from the surface to volume ratios of the plates.

C. Emanation Measurements

The emanation measurements were performed in a flow system (Reference 11 and Figure 1) using an alpha-scintillation detector and both pure helium and helium-hydrogen mixtures as carrier gases. The UO_2 samples, contained in alumina boats, were placed in a zircon tube and heated in a silicon carbide furnace. Temperatures were measured with platinum/platinum-10 percent rhodium thermocouples. The thoron activity was recorded automatically. The calibration of the apparatus, type and manufacturer of the commercial equipment used, and further details of the measurements are given in Appendix B.

TABLE 1. PHYSICAL PROPERTIES OF SINTERED UO_2 PLATES

% TD	Open Porosity (%)	β Activity (c/m/g x 10^{-5})	r (μ)
70.7	28.4	1.08	3.5
70.9	28.4	1.08	3.5
71.1	28.0	1.08	3.9
71.1	28.0	1.08	3.9
75.8	23.2	1.08	8.6
78.6	19.9	1.54	10.5
79.2	19.6	1.54	10.8
79.9	19.7	1.87	11.7
80.5	19.1	1.87	12.2
82.6	15.7	6.56	14.0
83.5	14.6	6.56	15.0
84.9	11.8	1.54	16.1
98.6	0	23.4	----
98.9	0	23.4	----
98.9	0	23.4	----

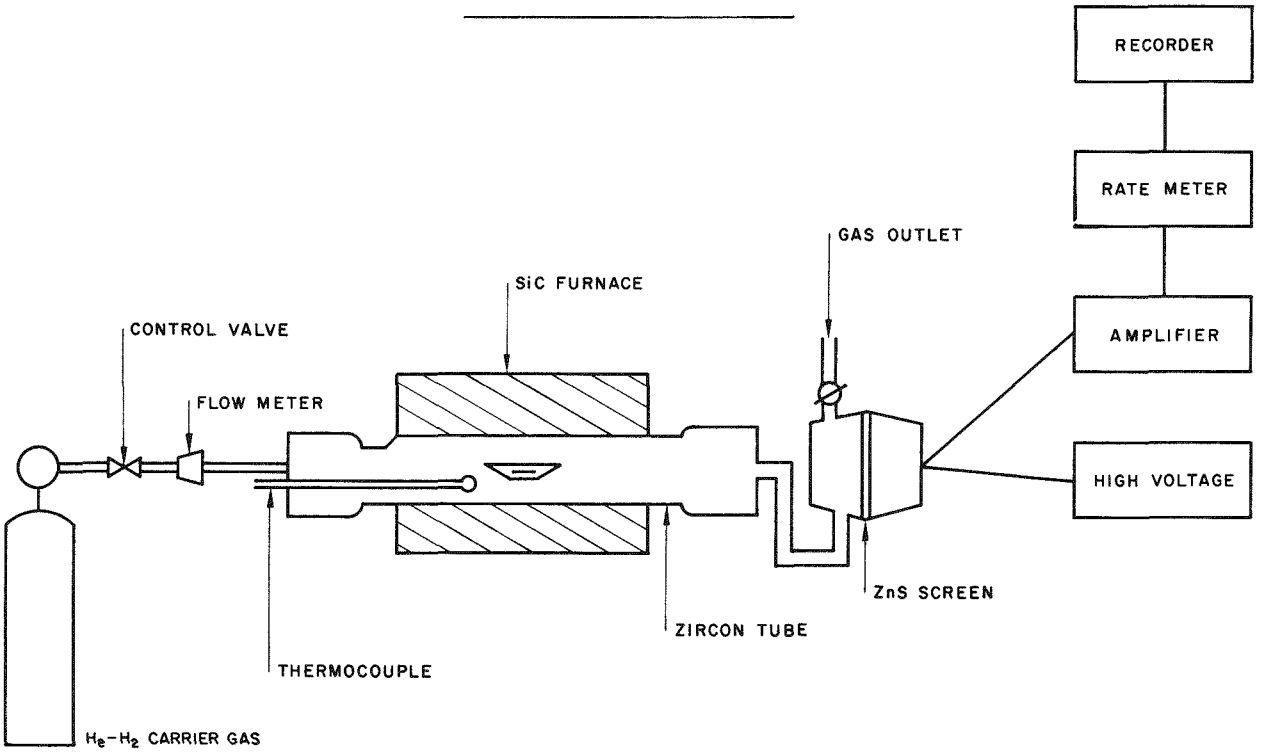

Figure 1. Schematic of Emanation Apparatus

IV. RESULTS

A. Thorium X Rejection

To calculate valid thoron diffusion coefficients from emanating power measurements, the radiothorium source compound must be homogeneously distributed throughout the whole solid, and this distribution should remain uniformly constant. In addition, the immediate precusor of thoron, thorium X

(Ra^{224}), should retain this uniform distribution. However, it has been observed that in many solids, including UO_2, the thorium X becomes non-uniformly redistributed at high temperatures (References 12 through 15). This phenomenon has been termed THORIUM X REJECTION by Bevan (Reference 12) and is an experimental factor limiting the quantitative application of thoron emanating power measurements to the study of diffusion problems. It is detected by high temperature isothermal increases in the thoron emanation with time followed by an excess surface activity at lower temperatures which decays near room temperature with the half-life of thorium X.

In the preliminary studies on sintered UO_2 powders and plates, pure helium was used as the carrier gas and thorium X rejection occurred. Definite increases in thoron emanation with time for the higher temperature isotherms were found as illustrated in Figure 2. In addition, the UO_2 samples oxidized slightly as indicated by color changes and weight increases on removal from the furnace after a heating run. With a helium-(5, 10%) hydrogen carrier gas mixture, the emanation of thoron was considerably lower than when helium alone was used. It is seen in Table 2 that this resulted in lower calculated diffusion coefficients and activation energies. Besides eliminating oxidation the addition of hydrogen to the helium carrier gas was also found to reduce drastically the amount of thorium X build-up on the UO_2 sample surfaces for the higher temperature isotherms. Only slight amounts of thorium X rejection were observed at 1450°C for the lowest density (71 to 76 percent TD) UO_2 plates and some of the sintered powder preparations. For these reasons the helium-hydrogen carrier gas mixture was used in all subsequent work.

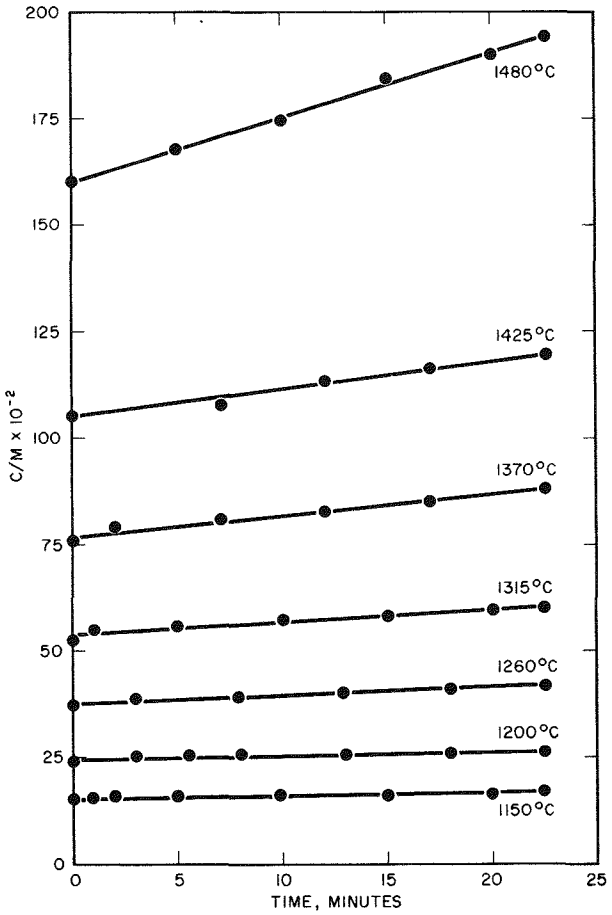

Figure 2. Isothermal Increase of Thoron Emanation with Time

B. Emanation Measurements

1. Sintered UO_2 Powders

Since previous thoron emanation measurements from metal oxides, including UO_2 (References 1, 5, and 12 through 22), were performed on powder samples, sintered UO_2 powder preparations were used for the initial experiments. The powders were first heated in hydrogen for 40 hours at 1750°C to stabilize the particle size distribution. The reproducibility of the emanation method was tested by measuring the same sample several times. In most cases the first measurement on a sample showed a greater amount of thoron evolution at the higher temperatures. This resulted in higher calculated high-temperature diffusion coefficients and activation energies than in subsequent runs. A small peak in the thoron emanation versus temperature curve was frequently observed around 600 to 900°C. Similar peaks were found by Anderson, et al., (Reference 13) for superstoichiometric UO_2 powders and were attributed to the reduction of UO_{2+x} to $UO_{2.0}$.

The thoron emanating power of a series of UO_2 powder preparations was measured, and diffusion

coefficients were calculated with Equation (3). An average particle radius of 5 microns has been found to be a reasonable estimate for similarly sintered oxide powders (Reference 19).

TABLE 2. THE EFFECT OF EXCESS OXYGEN ON $D_{Rn^{220}}$ IN SINTERED UO_2 PLATE

% TD	Sample	Carrier	Chemical Reaction	Temperature (°C)	D (cm^2/sec)	Q (kcal/mole)
78.6	$UO_{2.0}$ plate	Helium	Oxidation (weight gain)	1100-1450	1×10^{-14} - 2×10^{-12}	75
78.6	Oxidized $UO_{2.0}$ plate	He, 5% H_2	Reduction (weight loss)	1100-1450	7.5×10^{-16} - 3×10^{-13}	80
78.6	$UO_{2.0}$ plate	He, 5% H_2	None	1100-1450	2.7×10^{-15} - 5×10^{-14}	39.5
79.2	$UO_{2.0}$ plate	Helium	Oxidation (weight gain)	1100-1450	3×10^{-14} - 2×10^{-12}	82.5
79.2	Oxidized $UO_{2.0}$ plate	He, 5% H_2	Reduction (weight loss)	1100-1450	4.5×10^{-15} - 3×10^{-12}	60.6
79.2	$UO_{2.0}$ plate	He, 5% H_2	None	1100-1450	2.5×10^{-15} - 3×10^{-14}	35

The diffusion coefficients calculated from both 1-hour isothermal and continuous emanating power data are compared in Tables 3 and 4 over the temperature range 1000 to 1450°C. Only for the 1450°C isotherms was there a noticeable increase in the thoron emanation from some of the UO_2 powders. The initial emanating power values at 1450°C was used for these powders. Because this was the highest temperature studied, thorium X rejection should not have appreciably affected the calculated values of the diffusion coefficients.

TABLE 3. THE ISOTHERMAL EMANATION OF Rn^{220} FROM UO_2 POWDERS

Preparative Method	β Activity (c/m/g)	D (cm^2/sec) 1250°C	1350°C	1450°C	Q (kcal/mole)
Coprecipitation	1.00×10^5	2.1×10^{-14}	2.7×10^{-14}	4.8×10^{-14}	31.4
Coprecipitation	1.87×10^5	1.2×10^{-15}	2.3×10^{-15}	4.7×10^{-15}	38.3
Coprecipitation	1.21×10^6	3.5×10^{-16}	6.3×10^{-16}	2.1×10^{-15}	53.8

TABLE 4. THE CONTINUOUS EMANATION OF Rn^{220} FROM UO_2 POWDERS

Preparative Method	D (cm^2/sec) Coprecipitation	Coprecipitation	Coprecipitation	Coevaporation
β Activity (c/m/g)	1.54×10^5	6.56×10^5	6.56×10^5	2.34×10^6
Q (kcal/mole)	48.7	36.3	30.2	53.2
Temperature (°C)				
1000	1.1×10^{-15}	1.4×10^{-16}	1.6×10^{-16}	4.6×10^{-16}
1100	2.1×10^{-15}	2.0×10^{-16}	3.9×10^{-16}	1.4×10^{-15}
1200	5.8×10^{-15}	4.7×10^{-16}	8.8×10^{-16}	5.3×10^{-15}
1300	2.0×10^{-14}	1.1×10^{-15}	1.7×10^{-15}	3.0×10^{-14}
1400	5.3×10^{-14}	2.3×10^{-15}	2.9×10^{-15}	7.1×10^{-14}
1450	7.8×10^{-14}	2.9×10^{-15}	3.5×10^{-15}	8.5×10^{-14}

Reproducible data were obtained from a particular powder batch, but both calculated D values and activation energies varied from preparation to preparation. The different diffusion coefficients are most likely the result of differences in the average particle size of the various powders. The variation in activation energies is in agreement with previous studies on rare gas diffusion in UO_2 powders listed in Table 5 and can be attributed to differences in particle size distribution, particle shape, and amounts of excess oxygen. These factors will be discussed in a later section of this report.

TABLE 5. SUMMARY OF RARE GAS DIFFUSION STUDIES IN UO_2 POWDERS

Gas	Q (kcal/mole)	Temperature Range (°C)	Reference
Rn-220	30-54	1000-1450	---------
Rn-220	80-85	1150-1300	13,19
Rn-222	59.0	800-1400	20,21
Xe-133	46.0	1000-1500	23
Xe-133	34.0	550-1150	24
Xe-133	48.9	750-1150	25
Xe-133	40, 120	1000-1500	26
Xe-133	50, 70-80	600-1200	27
Kr-85	46.9	800-1500	28
Kr-85	65.5	1000-1500	29,30
Kr-85	73.8	1000-1500	29,30
Kr-85	70-80	1000-1450	31
He	46.0	700-1000	30,1

2. Low Density UO_2 Plates

In previous diffusion studies sintered UO_2 bodies have been considered as equivalent to an assembly of uniform spherical regions (References 1, 23, 26, 30, and 32). The controlling parameter is thus the radius of an equivalent hypothetical sphere and is calculated from the equation

$$r = 3 / Sd \qquad (5)$$

where

r = radius of equivalent sphere, cm
S = surface area, cm^2/g
d = density

The surface areas of four sintered UO_2 plates were directly measured by krypton gas adsorption, and the areas are plotted as a function of density in Figure 3. The surface area values for the remainder of the low density samples were interpolated from the curve in Figure 3. Photomicrographs of four oxide plates (71, 76, 79, and 85 percent TD) are shown in Figures 4 and 5. The decrease in pore volume with increasing density is apparent. It can also be readily seen that the assumption of an assembly of uniform spheres is incorrect and that the preparations instead contain pores of varying amounts, shapes, and sizes. These factors do not necessarily invalidate the quantitative application of the spherical model so long as the results are applied to bodies prepared by fabrication processes similar to those used for the present preparations.

Approximately 60 thoron emanation versus temperature curves were obtained on 12 low density sintered UO_2 plates. Some typical plots are shown in Figure 6. Diffusion coefficients were calculated with Equation (3); the particle radius values were calculated from Equation (5) and the surface area curve in Figure 3. The reproducibility and applicability of the emanation method to sintered bodies was tested by measuring each sample several times. In all cases the first measurement of a UO_2 plate showed a greater amount of thoron emanation, especially at the higher temperatures. As shown in Table 6, this resulted in higher calculated diffusion coefficients and activation energies than in subsequent runs. In addition, a small peak in the thoron emanation versus temperature curve was frequently observed

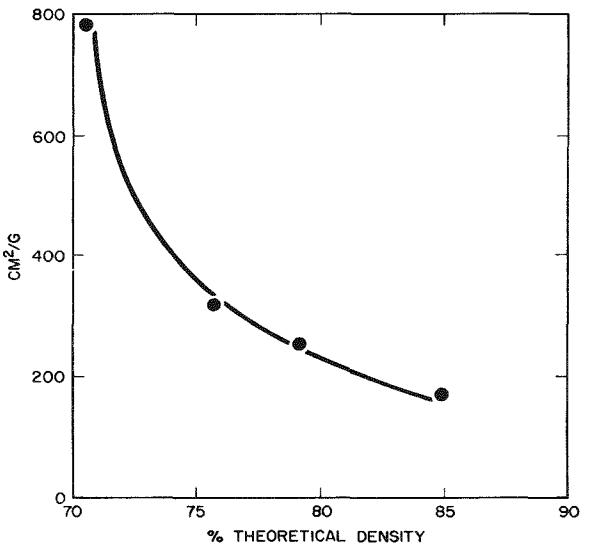

Figure 3. Surface Area of Sintered UO_2 Plates as a Function of Density

in the initial measurement around 600 to 900°C indicating that even these hydrogen-sintered UO_2 bodies contain traces of excess oxygen which noticeably influence their emanation behavior.

Neglecting the results of the first measurement on each sample, diffusion coefficients for Rn^{220} in low density UO_2 plates were calculated from both isothermal and continuous heating curves. The data obtained from 1-hour isotherms are given in Table 7. Isotherms at 1250, 1350, and 1450°C showed an essentially constant amount of thoron gas evolved at each temperature for the higher density (78 to 85 percent TD) plates, but there was a noticeable steady increase in the thoron emanation at 1450°C for the lower density (71 to 76 percent TD) plates. The initial emanating power values at 1450°C were used for these latter cases.

Because the isothermal measurements showed that emanation equilibrium was very quickly attained at each of the temperatures studied, the use of the more convenient continuous heating technique seemed justified. The extensive data acquired over the temperature range 1100 to 1450°C are tabulated in Appendix C. The calculated diffusion coefficients varied from 0.2×10^{-14} to 3×10^{-14} cm^2/sec at 1100°C to 0.2×10^{-13} to 4×10^{-13} cm^2/sec at 1450°C. No noticeable effect of radiothorium concentration on the emanation data is observed. However, both the isothermal (Table 7) and continuous heating measurements (Appendix C) indicate an over-all increase of activation energy with density. These emanation data were coded for CURF 1, a least squares fitting program for the Philco-2000 computer (Reference 33). Least squares analyses were performed on both the isothermal and continuous heating data points relating the variation with temperature of the diffusion coefficient of Rn^{220} in low density UO_2 plates. Over the temperature range 1100 to 1450°C the diffusion coefficient was represented by an equation of the form, $D = D_0 \exp(-Q/RT)$. The results of the machine computations are given in Table 8 and plotted in Figures 7, 8, and 9. The apparent increase in both activation energy (Q) and D_0 with density is clearly seen. Fair agreement was obtained between the isothermal and continuous heating data. From an overall least squares analyses of all the data points (Figure 9) the diffusion coefficient for Rn^{220} in sintered low density (71 to 85 percent TD) UO_2 plates can be represented by the equation,

$$D = 1 \times 10^{-8} \exp(-39{,}500/RT)$$

In some cases emanation measurements could be made on the sintered UO_2 powders and low density plates at temperatures as low as 400°C. Some typical results for the low density analyses are presented in Table 9. Log D versus 1/T plots for the 80 percent TD case (Figure 10) over the temperature range 400 to 1450°C gave three straight lines which intersected at temperatures of about 1100°C (T*) and 750°C (T**). Activation energies for these temperature ranges are listed in Table 10. This behavior is very similar to that of thoron in most oxide powders, including UO_2 powder (References 1, 13, 14, and 19), and the data are compared with some previous emanation work in Table 11. In addition, two intersecting straight lines on a log diffusion coefficient versus temperature plot have been found for the diffusion of Kr^{85} and Xe^{133} from irradiated UO_2 (References 1, 31, 32, and 35). In all cases a high activation energy (40 to 89 kcal/mole) for diffusion is observed at high temperatures; at low temperatures a much lower energy (8 to 38 kcal/mole) is observed.

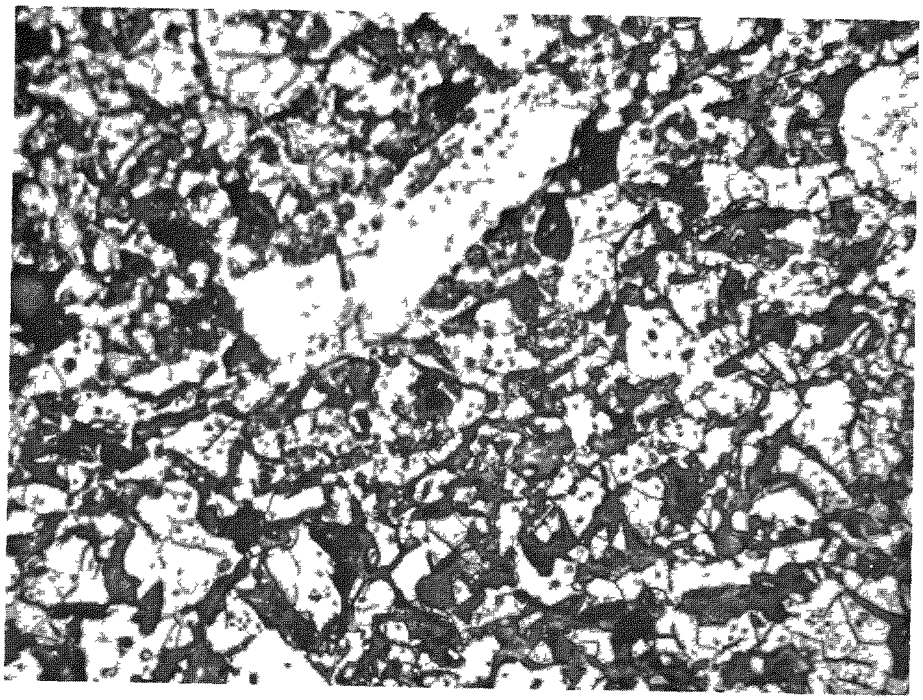

A. 71.1% TD; Etched

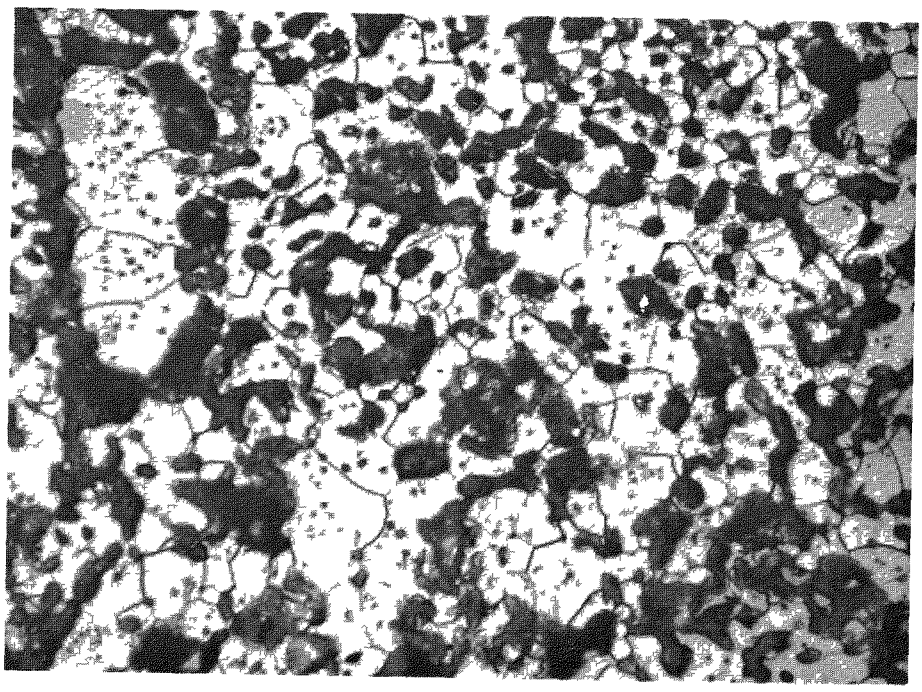

B. 75.8% TD; Etched

Figure 4. Microstructure of Low Density UO_2 Plates (500X)

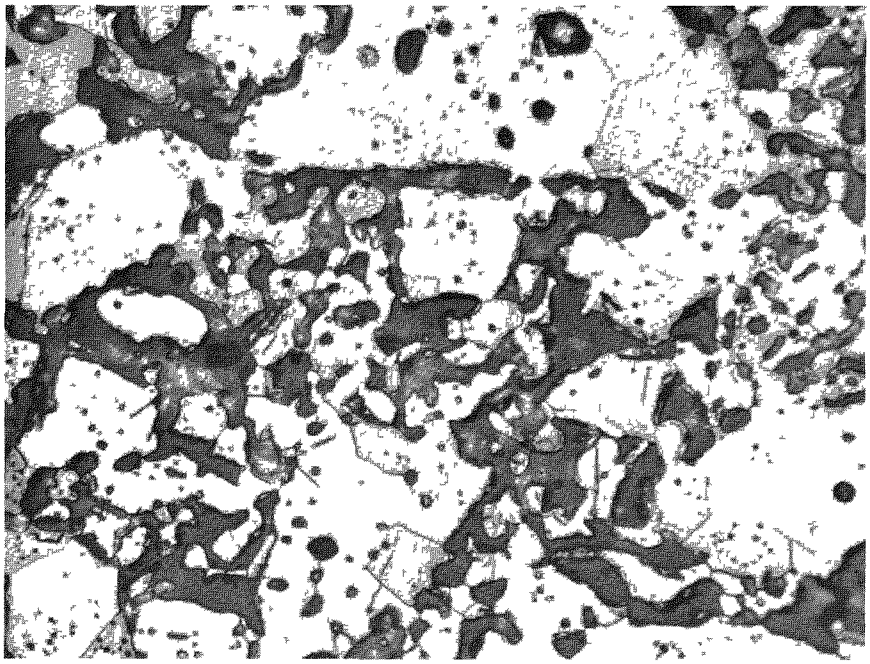

A. 79.2% TD; Etched

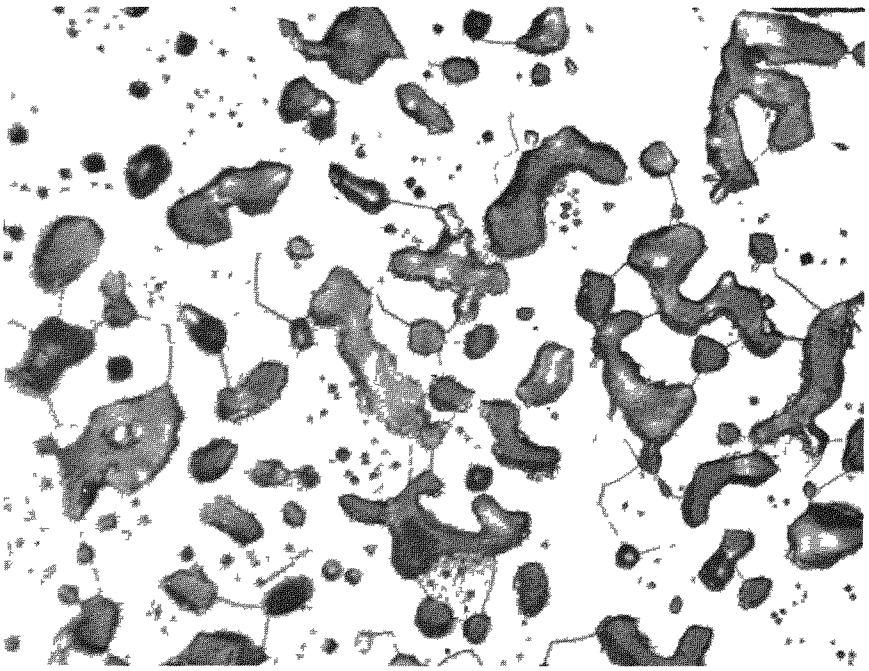

B. 84.9% TD; Etched

Figure 5. Microstructure of Low Density UO_2 Plates (500X)

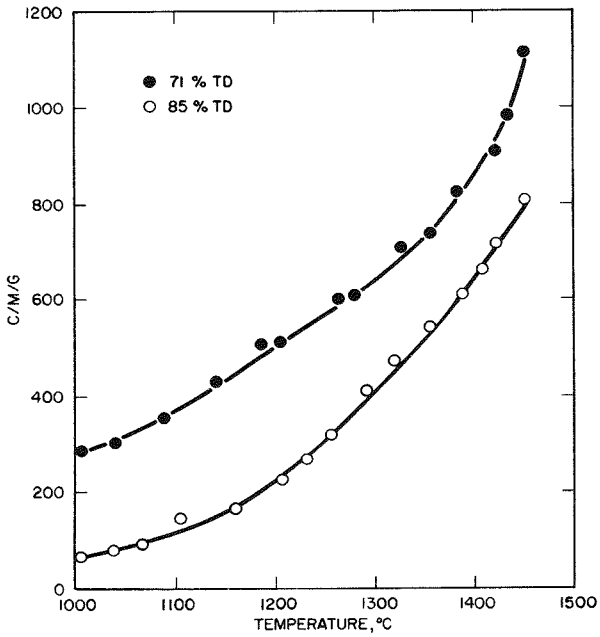

Figure 6. Thoron Emanation Activity from Low Density UO_2 Plates

The several straight lines and different activation energies have been interpreted as representing at least two independent diffusion processes with a transition taking place in the vicinity of the Tammann temperature (References 1, 13, 14, and 19). The Tammann temperature has been defined as the temperature at which the diffusion coefficient is 10^{-14} to 10^{-17} cm^2/sec or a temperature equal to 0.5 times the melting point on the Kelvin scale (Reference 1). If α represents the ratio of the absolute temperature of an ionic solid to its melting point on the Kelvin scale, surface mobility of lattice units is believed to become appreciable at above $\alpha = 0.3$, whereas lattice diffusion requires $\alpha = 0.5$ (the Tammann temperature) or higher (References 1 and 36). The closeness with which the T* and T** temperatures (intersection of straight lines on log D versus 1/T plot) approach these ratios (Table 5), the diffusion coefficient values of 1×10^{-15} to 3×10^{-15} cm^2/sec at T*, and the different activation energies observed for the high and low temperature ranges, all suggest that the emanation of thoron from sintered low density UO_2 plates involves lattice diffusion at α of about 0.5, diffusion in a surface layer for α between 0.3 to 0.5, and a possible third process in which the thoron escapes through such crystal defects as pores and cracks of molecular dimensions (References 13, 14, 18, and 19).

TABLE 6. REPRODUCIBILITY OF THE EMANATION OF Rn^{220} FROM UO_2 PLATES

	D (cm^2/sec)					
% TD	75.75	75.75	75.75	79.9	79.9	79.9
r (μ)	8.6	8.6	8.6	11.7	11.7	11.7
Run No.	1	2	3	1	2	3
Q (kcal/mole)	39.8	33.9	34.3	71.5	46.2	47.2
Temperature (°C)						
1100	1.9×10^{-14}	7.5×10^{-15}	7.6×10^{-15}	1.1×10^{-15}	2.7×10^{-15}	2.3×10^{-15}
1200	2.7×10^{-14}	1.3×10^{-14}	1.4×10^{-14}	3.8×10^{-15}	8.1×10^{-15}	7.7×10^{-15}
1300	4.7×10^{-14}	2.4×10^{-14}	2.6×10^{-14}	2.0×10^{-14}	2.5×10^{-14}	2.6×10^{-14}
1400	7.7×10^{-14}	4.5×10^{-14}	5.0×10^{-14}	9.5×10^{-14}	5.5×10^{-14}	5.3×10^{-14}
1450	1.5×10^{-13}	7.3×10^{-14}	7.7×10^{-14}	1.5×10^{-13}	7.5×10^{-14}	7.0×10^{-14}

3. High Density UO_2 Plates

When the sintered UO_2 bodies approach the theoretical density, a diffusion model based on geometric dimensions is more exact than the equivalent sphere treatment. The surface areas of the as-sintered high density UO_2 plates were measured by ethane gas adsorption and were found to correspond to the geometric areas (roughness factor of about one). Photomicrographs of a typical 99 percent TD UO_2 plate are given in Figure 11. For the most part cross-sections of these samples showed dense, large grains with very little porosity (Figure 11A), but there were a few isolated areas that contained noticeable porosity (Figure 11B).

TABLE 7. THE ISOTHERMAL EMANATION OF Rn^{220} FROM LOW DENSITY UO_2 PLATES

% TD	r (μ)	β Activity (c/m/g)	D (cm^2/sec) 1250°C	1350°C	1450°C	Q (kcal/mole)
70.7	3.5	1.08×10^5	9.7×10^{-15}	1.5×10^{-14}	2.7×10^{-14}	30.7
70.9	3.5	1.08×10^5	8.9×10^{-15}	1.4×10^{-14}	2.9×10^{-14}	33.6
71.1	3.9	1.08×10^5	1.2×10^{-14}	2.0×10^{-14}	4.3×10^{-14}	37.3
71.1	3.9	1.08×10^5	1.1×10^{-14}	2.0×10^{-14}	4.2×10^{-14}	36.3
75.8	8.6	1.08×10^5	2.5×10^{-14}	5.5×10^{-14}	1.1×10^{-13}	39.5
78.6	10.5	1.54×10^5	7.3×10^{-14}	1.7×10^{-13}	3.1×10^{-13}	37.5
79.9	11.7	1.87×10^5	1.5×10^{-14}	4.1×10^{-14}	7.1×10^{-14}	41.2
80.5	12.2	1.87×10^5	1.7×10^{-14}	4.9×10^{-14}	8.9×10^{-14}	42.4
82.6	14.0	6.56×10^5	2.2×10^{-14}	5.9×10^{-14}	1.2×10^{-13}	42.0
84.9	16.1	1.54×10^5	3.2×10^{-14}	9.4×10^{-14}	2.4×10^{-13}	51.4

TABLE 8. LEAST SQUARES ANALYSES OF THORON EMANATION DATA FROM UO_2 PLATES

Range (% TD)	D_o	Q (kcal/mole)	Std Error Deviation (σ)	Max Abs Error (μ)	Number of Specimens	Number of Runs	Number of Points
			Continuous Heating (1100-1450°C)				
71	2.2×10^{-10}	30.8	0.27	0.82	4	6	30
76	4.5×10^{-10}	30.4	0.11	0.17	1	2	10
79	6.5×10^{-9}	35.2	0.51	0.11	2	13	65
80	5.0×10^{-8}	45.8	0.90	0.16	2	3	15
83-85	7.2×10^{-7}	53.1	0.19	0.45	3	5	25
71-85	7.5×10^{-9}	39.0	0.68	1.27	12	29	145
99	0.13	80.0	0.40	0.94	3	8	40
			Isotherms (1250-1450°C)				
71	2.9×10^{-10}	31.2	0.18	0.29	4	4	12
76-79	1.5×10^{-8}	38.8	0.53	0.56	2	2	6
80	2.0×10^{-8}	42.4	0.13	0.22	2	2	6
83-85	2.2×10^{-7}	48.2	0.27	0.39	2	2	6
71-85	1.2×10^{-8}	40.0	0.63	1.09	10	10	30
99	4.9×10^{-5}	51.5	0.25	0.51	3	3	9

The thoron emanating power of the three high density UO_2 plates was measured, and diffusion coefficients were calculated with Equation (4). Again the first measurement on a sample showed a greater amount of thoron emanation, consequently, a higher apparent activation energy for the high temperature regions. The effect was generally not as pronounced as for the sintered UO_2 powders and low density plates but does indicate that even the high density hydrogen-sintered UO_2 wafers (as prepared) contain traces of excess oxygen. To test this hypothesis, four hydrogen-sintered (1750°C), 95 percent TD UO_2 pellets were re-heated in hydrogen for 4 hours at 1500°C and then exposed to the atmosphere at room temperature. The outer surface (estimated to be <0.008 cm) of the compacts was dissolved off in hot phosphoric acid under an argon atmosphere, and the solutions were polarographically analyzed for U(VI). The amount of U(VI) measured in three of the samples corresponded to O/U ratios of 2.002 to 2.003.

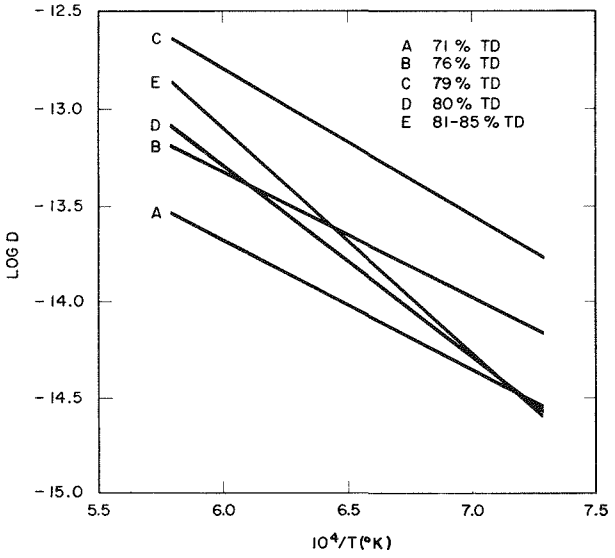

Figure 7. Variation of D with Temperature: Continuous Heating Curves

Diffusion coefficients for Rn^{220} in high density UO_2 plates calculated from both 1-hour isothermal and continuous heating curves are compared in Table 12. In contrast to the measurements on sintered UO_2 powders and low density plates where the recorded isotherms showed an essentially constant unvarying evolution of thoron gas at each temperature, the high temperature isothermal gas evolution from the high density samples was, at times, in spasmodic spurts. This effect may have been caused by the closed pores present in the samples (Figure 11B). Excess thoron gas could accumulate in these closed pores, and at the higher temperatures any pore movement to the surface or, more likely, to grain boundaries could result in a temporary enhanced gas release.

No over-all increase in thoron emanation with time, corresponding to thorium X rejection, was noted, but the recorded curve was jagged and jerky. Consequently, diffusion coefficients calculated from the isothermal data can only be regarded as estimates. The continuous heating curves, however, were smooth and reproducible. Both the isothermal and continuous heating measurements yielded thoron diffusion coefficients and activation energies that were higher than those obtained for the sintered UO_2 powders and low density plates. The calculated diffusion coefficients varied from 0.8×10^{-13} to 4.7×10^{-13} cm^2/sec at 1200°C to 0.9×10^{-11} to 1.5×10^{-11} cm^2/sec at 1450°C and agree with estimated values found previously in sintered high density UO_2 grains (References 13 and 19). In this connection other workers (Reference 34) have reported orders of magnitude increases (10^{-14} to 10^{-13} and 10^{-12} cm^2/sec) in the 1400°C diffusion coefficient of Xe^{133} in lightly irradiated UO_2 bodies with an increase in the fabricated density from 91 to 97 percent TD. Least squares analyses performed on the data are compared

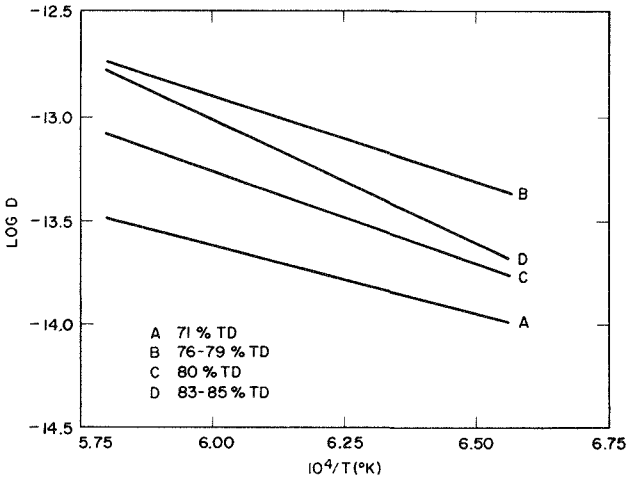

Figure 8. Variation of D with Temperature: Isothermal Data

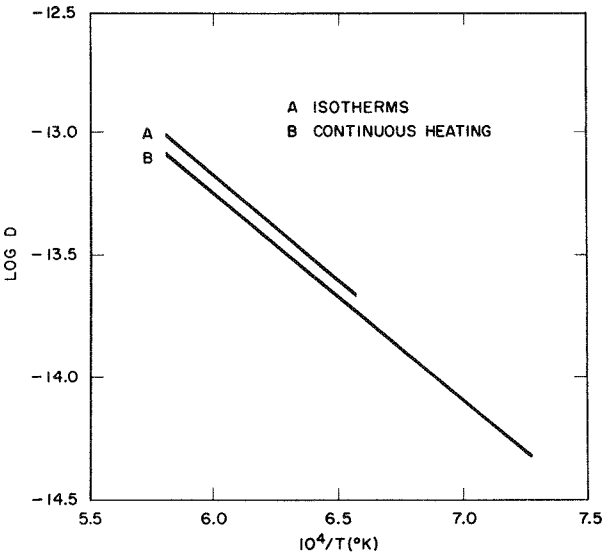

Figure 9. Variation of D with Temperature: Over-all Least Square Lines

TABLE 9. THE DIFFUSION OF Rn^{220} FROM LOW DENSITY UO_2 PLATES

% TD	79.9	80.5	82.6	83.5	84.9
r (μ)	11.7	12.2	14.0	15.0	16.1
Temperature (°C)					
400	3.9×10^{-18}	1.6×10^{-17}	1.4×10^{-17}	1.8×10^{-18}	1.0×10^{-17}
500	2.5×10^{-17}	2.6×10^{-17}	3.3×10^{-17}	1.4×10^{-17}	1.5×10^{-17}
600	4.7×10^{-17}	4.2×10^{-17}	5.1×10^{-17}	2.9×10^{-17}	2.9×10^{-17}
700	7.0×10^{-17}	7.4×10^{-17}	6.8×10^{-17}	3.9×10^{-17}	6.6×10^{-17}
800	1.5×10^{-16}	1.6×10^{-16}	1.2×10^{-16}	6.4×10^{-17}	2.1×10^{-16}
900	5.0×10^{-16}	4.5×10^{-16}	3.2×10^{-16}	1.9×10^{-16}	5.1×10^{-16}
1000	1.3×10^{-15}	1.4×10^{-15}	1.3×10^{-15}	7.9×10^{-16}	9.2×10^{-16}
1100	2.7×10^{-15}	2.9×10^{-15}	2.8×10^{-15}	1.6×10^{-15}	2.7×10^{-15}
1200	8.1×10^{-15}	8.8×10^{-15}	9.0×10^{-15}	8.8×10^{-15}	9.7×10^{-15}
1300	2.5×10^{-14}	2.7×10^{-14}	3.1×10^{-14}	4.2×10^{-14}	3.4×10^{-14}
1400	5.5×10^{-14}	5.8×10^{-14}	8.0×10^{-14}	1.1×10^{-13}	8.7×10^{-14}
1450	7.5×10^{-14}	8.0×10^{-14}	1.1×10^{-13}	1.5×10^{-13}	1.3×10^{-13}

with the results from the low density UO_2 plates in Table 8 and plotted in Figure 12. The apparent increase in both activation energy and D_0 value with density is again indicated. Over the temperature range 1200 to 1450°C the diffusion coefficient for Rn^{220} in sintered high density UO_2 plates can be represented by the equation,

$$D = 0.13 \exp(-79{,}960/RT).$$

The high activation energy compares favorably with that found for the release of the fission gases Xe and Kr from irradiated high density ($\gtrsim$95 percent TD) sintered UO_2 masses listed in Table 13.

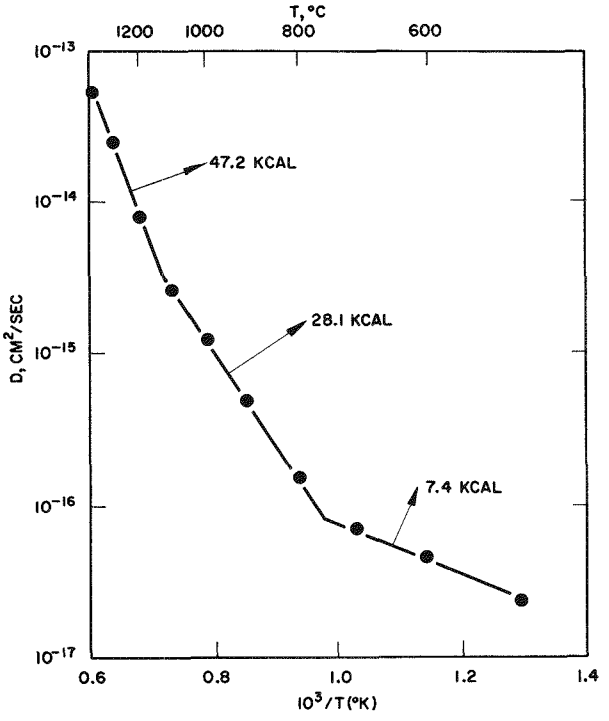

Figure 10. Variation of D with Temperature in an 80 Percent TD UO_2 Plate

In general, thoron evolution from the high density UO_2 plates could not be measured below 1200°C because of the small surface area of the samples. In a few cases measurements were made at temperatures as low as 1000°C, and two intersecting straight lines were obtained on a log diffusion coefficient versus reciprocal temperature plot. The results are compared with some British studies on high density sintered UO_2 grains in Table 14. The data are limited and show scatter, but the lines do intersect near the Tammann temperature (α = 0.45 to 0.50). This, plus the fact that two different activation energies were observed, confirms the results found for the sintered UO_2 powders and low density plates in indicating that the emanation of Rn^{220} from UO_2 involves at least two types of diffusion processes.

TABLE 10. THE EMANATION OF Rn^{220} FROM SINTERED LOW DENSITY UO_2 PLATES, 400 TO 1450°C

% TD	r (μ)	T* (°K)	D at T* (cm^2/sec)	Q_1 (Above T*) (kcal/mole)	Q_2 (Below T*) (kcal/mole)	T** (°K)	D at T** (cm^2/sec)	Q_3 (Below T**) (kcal/mole)
79.9	11.7	1383	3.0×10^{-15}	47.2	28.1	1025	8.5×10^{-17}	7.4
79.9	11.7	1373	2.1×10^{-15}	46.2	26.9	1010	6.2×10^{-17}	9.0
80.5	12.2	1385	3.4×10^{-15}	44.7	29.3	1037	9.4×10^{-17}	7.9
82.6	14.0	1359	2.4×10^{-15}	49.5	30.9	1049	8.4×10^{-17}	5.6
83.5	15.0	1340	1.3×10^{-15}	57.2	31.8	1064	5.8×10^{-17}	7.6
83.5	13.0	1350	1.5×10^{-15}	53.2	30.5	1055	6.5×10^{-17}	5.3
84.9	16.1	1323	1.3×10^{-15}	52.0	19.9	926	4.7×10^{-17}	11.7

T*, T** } intersection of straight lines on log D versus 1/T plot

TABLE 11. SUMMARY OF THORON EMANATION STUDIES ON OXIDES

Oxide	T* (°K)	α	D at T* (cm^2/sec)	Q_1 (Above T*) (kcal/mole)	Q2 (Below T*) (kcal/mole)	Reference
Fe_2O_3	910	0.51	0.6×10^{-14}	42.2	8.4	16, 18
Cr_2O_3	1110	0.51	1.7×10^{-14}	49.5	12.7	16, 18
Al_2O_3	1198	0.52	2.8×10^{-14}	60.6	7.4	18
UO_2	1363	0.45	2×10^{-15}	50	28	---
ThO_2	1473	0.44	----	61.3	31.5	12, 15

T* intersection of straight lines on log D versus 1/T plot

V. DISCUSSION

Although these measurements have been made on materials undamaged by irradiation, they should none the less be useful in determining which factors govern rare gas diffusion in slightly irradiated UO_2. The profound increase in the gas diffusion rates caused by even traces of excess oxygen has been well documented (References 1, 13, 19, 23, 25, 26, 27, 31, 32, and 37 to 40). The variation in activation energy for the diffusion of thoron in UO_2 powders is not surprising, especially in view of the results of previous rare gas diffusion studies (Table 5). UO_2 powders usually have a wide particle size distribution, vary in shape, and are very susceptible to oxygen pickup even at room temperature. Fine powders can sinter readily during a diffusion anneal. These factors have recently been reviewed by Matzke and Lindner (Reference 27) who used them to interpret the apparent activation energies for Xe^{133} in UO_2 powders (50 to 80 kcal/mole).

Both the isothermal and continuous heating emanating power data indicate an increase in activation energy and D_o with density for the diffusion of Rn^{220} in sintered UO_2 plates. This may be due to unappreciated and uncontrolled experimental and material variables, e.g., the different methods of incorporating the radiothorium in the UO_2 samples (coprecipitation versus coevaporation). Treatment of the low density plates as an assembly of uniform spheres is over simplified. The photomicrographs (Figures 4 and 5) show that these oxide plates have a rather broad grain size distribution and many of the grain radii are considerably smaller and larger than the fictitious, ideal radius calculated from the

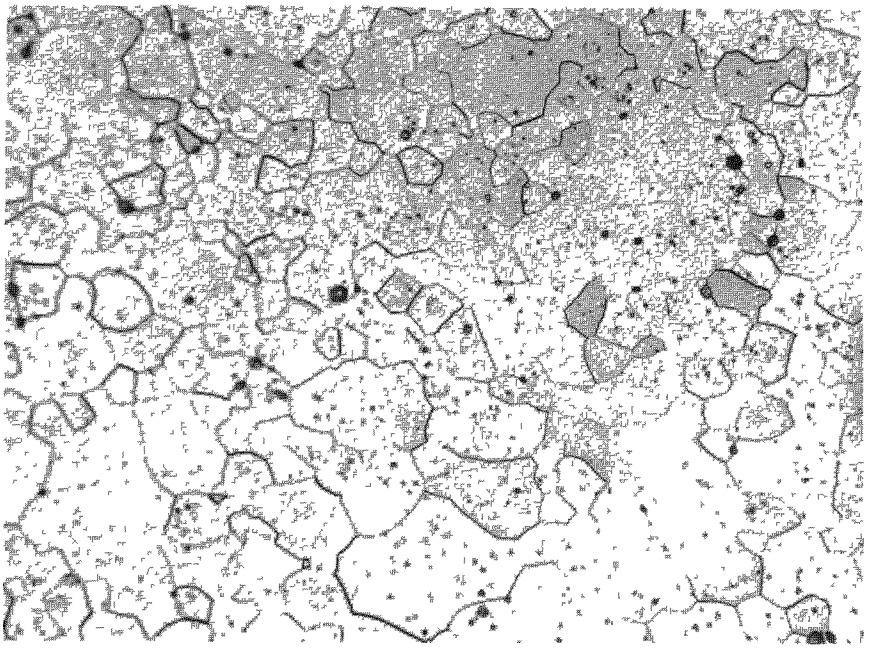

A. Etched

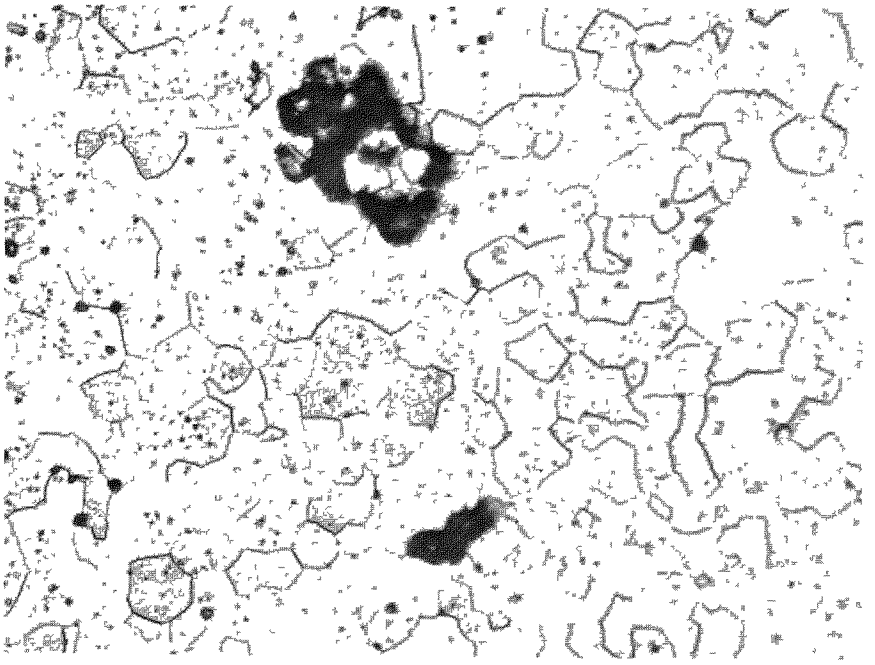

B. Etched

Figure 11. Microstructure of a 98.9 Percent TD UO_2 Plate (500X)

TABLE 12. THE EMANATION OF Rn^{220} FROM HIGH DENSITY UO_2 PLATES

% TD	D (cm^2/sec) 1200°C	1250°C	1300°C	1350°C	1400°C	1450°C	Q (kcal/mole)
			Continuous Heating				
98.6	8.3×10^{-14}	1.9×10^{-13}	4.6×10^{-13}	1.1×10^{-12}	2.9×10^{-12}	1.5×10^{-11}	83.2
98.6	2.1×10^{-13}	3.5×10^{-13}	7.2×10^{-13}	1.7×10^{-12}	4.8×10^{-12}	8.5×10^{-12}	86.0
98.6	4.7×10^{-13}	7.2×10^{-13}	1.4×10^{-12}	3.0×10^{-12}	5.6×10^{-12}	9.0×10^{-12}	64.0
98.9	3.4×10^{-13}	5.6×10^{-13}	1.2×10^{-12}	2.6×10^{-12}	5.3×10^{-12}	1.2×10^{-11}	79.3
98.9	2.9×10^{-13}	4.9×10^{-13}	9.7×10^{-13}	2.1×10^{-12}	6.0×10^{-12}	1.4×10^{-11}	88.0
98.9	1.2×10^{-13}	2.7×10^{-13}	6.3×10^{-13}	1.4×10^{-12}	2.8×10^{-12}	1.5×10^{-11}	77.6
98.9	2.4×10^{-13}	4.2×10^{-13}	9.7×10^{-13}	2.0×10^{-12}	4.0×10^{-12}	1.1×10^{-11}	75.0
98.9	3.2×10^{-13}	4.9×10^{-13}	1.0×10^{-12}	2.3×10^{-12}	5.9×10^{-12}	1.3×10^{-11}	72.1
			Isotherms				
98.6	----------	1.7×10^{-12}	----------	3.5×10^{-12}	----------	1.1×10^{-11}	53.8
98.9	----------	2.2×10^{-12}	----------	6.6×10^{-12}	----------	2.1×10^{-11}	57.9
98.9	----------	2.6×10^{-12}	----------	6.4×10^{-12}	----------	1.6×10^{-11}	49.8

surface area measurements. In addition, none of the grain boundary area is measured by the gas adsorption (BET) technique, and these short-circuit diffusion paths would further complicate the model. Finally, there is the possibility of some thoron adsorption and surface retention at the lower temperatures. However, the good agreement between the isothermal and continuous heating measurements on the low density plates tends to support the applicability of the equivalent sphere model. The observed increases in activation energy and D_0 values with density may, therefore, be real. Finally the high activation energy (80 kcal/mole) found for thoron diffusion in the 99 percent TD UO_2 plates is in good agreement with previous studies on rare gas diffusion from irradiated high density UO_2 masses (Table 14). The results of this investigation, therefore, supplement previous experimental work on the evolution of fission gases from slightly irradiated UO_2.

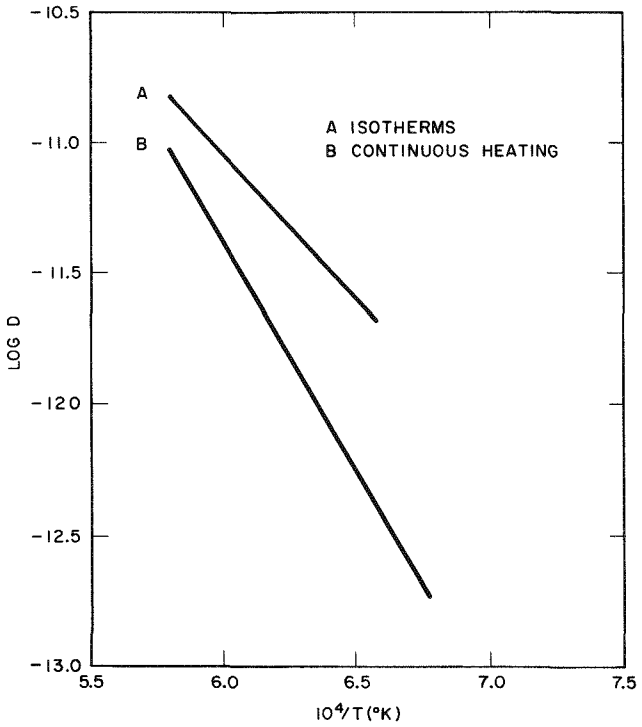

Figure 12. Variation of D with Temperature in a 99 Percent TD UO_2 Plate

VI. SUMMARY AND CONCLUSIONS

1) Both oxidation and thorium X rejection occurred in UO_2 powders and plates when pure helium was used as the carrier gas. The addition of hydrogen to the helium eliminated oxidation and drastically reduced the amount of thorium X build-up on the UO_2 sample surfaces. In the helium-hydrogen carrier gas mixture thorium X rejection

TABLE 13. SUMMARY OF RARE GAS DIFFUSION STUDIES IN SINTERED HIGH DENSITY UO_2

Gas	Q (kcal/mole)	Temperature Range (°C)	Reference
Rn-220	80.0	1200-1450	---------
Rn-220	80-85	1150-1300	13, 19
Xe-133	71.7	800-1300	30
Xe-133	76.0	1000-1450	1
Xe-133	90,120	1000-1500	26
Xe-133	83-115	1200-1550	38
Xe-133	92.0	1000-1600	41
Kr-85	67.0	800-1450	1
Kr-85	58.5	1100-1575	35
Kr-85	65.5	1000-1500	29, 30
Kr-85	70-80	1000-1450	31
Xe-Kr	~70	900-1900	37

TABLE 14. THE EMANATION OF Rn^{220} FROM SINTERED HIGH DENSITY UO_2, 1000 TO 1450°C

T* (°K)	α	D at T* (cm^2/sec)	Q_1 (Above T*) (kcal/mole)	Q_2 (Below T*) (kcal/mole)
1428(1)	0.47	$\sim 3 \times 10^{-13}$	80-85	40
1377	0.45	2.0×10^{-14}	77.6	44.9
1429	0.47	3.5×10^{-14}	83.2	45.6
1510	0.50	4.2×10^{-13}	79.3	25.1
1524	0.50	4.2×10^{-13}	88.0	31.0

(1) References 13 and 19

was not observed until 1450°C and then only in the lowest density (71 to 76 percent TD) UO_2 plates and some of the powder preparations. Excess oxygen was found to increase the thoron diffusion rates in sintered UO_2 powders and plates.

2) Low density UO_2 plates were considered equivalent to a collection of spheres for diffusion coefficient calculations. An apparent increase in both activation energy and D_o with density was observed. Good agreement was obtained between the isothermal and continuous heating data. From an over-all least squares analysis of all the data points the diffusion coefficient for Rn^{220} in sintered low density (71 to 85 percent TD) UO_2 plates can be represented by the equation,

$$D = 1 \times 10^{-8} \exp(-39{,}500/RT),$$ over the temperature range 1100 to 1450°C.

3) For the very high density (99 percent TD) UO_2 plates a diffusion model based on geometric dimensions was used. Both the isothermal and continuous heating measurements yielded higher thoron diffusion coefficients, and activation energies then were found for the sintered UO_2 powders and low density plates. Over the temperature range 1200 to 1450°C, the diffusion coefficient for Rn^{220} in sintered high density UO_2 plates can be represented by the equation,

$$D = 0.13 \exp(-79{,}960/RT).$$

4) For some samples the thoron emanating power could be measured at temperatures as low as 400°C. Log D versus 1/T plots from 400 to 1450°C gave three intersecting straight lines. A high activation energy was observed at high temperatures and at lower temperatures, lower energies. The lines intersect near the Tammann temperature and indicate that the emanation of Rn^{220} from UO_2 involves several diffusion processes.

APPENDIX A. SAMPLE PREPARATION AND STANDARDIZATION

The uranium oxide samples were indexed with Th^{228} by two techniques. In both processes tracer amounts (5-100 μ c/g UO_2) of radiothorium were added to uranyl nitrate solutions. In a coprecipitation procedure the uranium was precipitated as ammonium diuranate, ignited to U_3O_8 in air at 500°C, and reduced with hydrogen to UO_2 at 800°C. In a coevaporation method the thorium-uranyl nitrate solution was evaporated to uranyl nitrate hexahydrate which was pyrolyzed to UO_3 in electrically heated (200 to 400°C) porcelain ware. The coarse UO_3 was milled for 16 hours in a Zircaloy-2 ball mill. The milled UO_3 was placed in platinum boats and reduced with hydrogen to UO_2 at 800°C. Both types of tagged UO_2 preparations were further homogenized by annealing them in hydrogen for 40 hours at 1750°C. After being lightly ground in a mortar and pestle, the coprecipitated oxide preparations were mixed with one w/o Carbowax 20M (polyethylene glycol) and pressed into plates at 20 to 30 tsi. The green compacts were sintered in hydrogen at 1400 to 1750°C and the low density (71 to 85 percent TD) plates resulted. The oxide powder prepared by coevaporation was milled for 20 hours with uranium slugs in a rubber-lined metal mill. The comminuted powder was agglomerated with the organic binder, pressed into plates at 15 tsi, and sintered in hydrogen for 16 hours at 1750°C to produce the very high density (99 percent TD) wafers.

The barium stearate standard was prepared by adding a hot sodium stearate solution (6 g sodium stearate/250 ml water) to a barium chloride solution (2 g $BaCl_2 \cdot 2H_2O$/100 ml water) containing radiothorium (Reference 8). The precipitate was filtered, washed with distilled water, and dried in a vacuum oven at 55°C for 36 hours. The relative rates of formation of thoron gas in the barium stearate and each UO_2 powder preparation was determined by measurement of their beta activities in sealed aluminum containers after radioactive equilibrium had been attained (References 5 and 7). A beta-proportional counter with a 113 mg aluminum absorber and a Bi^{210} standard was used. The relative rates of escape of the thoron gas from the barium stearate and UO_2 were then determined in the flow system and the emanating power of the UO_2 was calculated with Equation (1). At least 4 weeks (more often longer) elapsed between a heating run on a particular sample.

APPENDIX B. EMANATION APPARATUS

A schematic diagram of the continuous flow apparatus is shown in Figure 1. The UO_2 samples, contained in alumina boats, were placed in a zircon tube which in turn was enclosed in a silicon carbide furnace. The furnace was a Brinkmann-Heraeus, Type S 40/3; its temperature could be varied manually with a powerstat and regulated to within ± 1°C with a Bristol pyrometer controller. A heating rate of 0.5°C/minute was used for the 950 to 1450°C temperature range. Temperatures were measured with platinum/platinum-10% rhodium thermocouples. A metal adapter on the furnace tube permitted the insertion of thermocouples directly above the UO_2 samples. These inner thermocouples were encased in ceramic protection tubes which were gas-tight up to 1500°C. The zircon tube immediately led to a zinc sulfide alpha scintillation probe (Baird-Atomic Model 870) which was entirely encased in an outer metal covering to prevent the escape of any radioactive species from the system. The alpha probe was connected to a Baird-Atomic, Inc., regulated high voltage power supply (Model 318) and a general purpose amplifier (Baird-Atomic Model 412). The alpha activity was counted with a precision dual-purpose ratemeter (Baird-Atomic Model 412) which simultaneously provided both logarithmic and linear readings. A time constant of 30 sec and a signal of 20 mv was used for most of the measurements. The alpha activity was plotted as a function both of high voltage and carrier gas flow rate. The optimum voltage and gas flow rate were found to lie on a plateau where the alpha activity was relatively insensitive to changes in either of these factors. Helium-(5, 10%) hydrogen mixtures were used as carrier gases and the flowrate was controlled with a Brooks Rotameter. A by-pass line allowed the "active deposit" background to be measured after each run without interruption of the gas flow.

APPENDIX C. THORON DIFFUSION COEFFICIENTS IN LOW DENSITY UO_2 PLATES

Density (% TD)	r (μ)	β Activity (c/m/g)	D (cm^2/sec) 1100°C	1200°C	1300°C	1400°C	1450°C	Q (kcal/mole)
70.7	3.5	1.08×10^5	4.1×10^{-15}	6.8×10^{-15}	1.1×10^{-14}	2.0×10^{-14}	3.3×10^{-14}	27.7
70.7	3.5	1.08×10^5	3.1×10^{-15}	5.6×10^{-15}	8.9×10^{-15}	1.5×10^{-14}	2.4×10^{-14}	25.1
70.9	3.5	1.08×10^5	4.0×10^{-15}	6.6×10^{-15}	1.1×10^{-14}	2.0×10^{-14}	3.5×10^{-14}	25.3
70.9	3.5	1.08×10^5	2.8×10^{-15}	4.9×10^{-15}	8.0×10^{-15}	1.4×10^{-14}	2.2×10^{-14}	27.4
71.1	3.9	1.08×10^5	2.9×10^{-15}	5.3×10^{-15}	1.1×10^{-14}	2.2×10^{-14}	4.8×10^{-14}	40.6
71.1	3.9	1.08×10^5	2.7×10^{-15}	5.3×10^{-15}	1.2×10^{-14}	2.8×10^{-14}	6.4×10^{-14}	41.6
75.8	8.6	1.08×10^5	7.5×10^{-15}	1.3×10^{-14}	2.4×10^{-14}	4.5×10^{-14}	7.3×10^{-14}	33.9
75.8	8.6	1.08×10^5	7.6×10^{-15}	1.4×10^{-14}	2.6×10^{-14}	5.0×10^{-14}	7.7×10^{-14}	34.3
78.6	10.5	1.54×10^5	2.0×10^{-14}	4.9×10^{-14}	9.3×10^{-14}	2.5×10^{-13}	4.2×10^{-13}	39.5
78.6	10.5	1.54×10^5	1.8×10^{-14}	4.9×10^{-14}	1.1×10^{-13}	1.5×10^{-13}	1.7×10^{-13}	27.6
78.6	10.5	1.54×10^5	7.1×10^{-15}	2.0×10^{-14}	4.0×10^{-14}	6.5×10^{-14}	8.3×10^{-14}	31.0
78.6	10.5	1.54×10^5	5.7×10^{-15}	2.2×10^{-14}	5.6×10^{-14}	8.5×10^{-14}	1.2×10^{-13}	35.2
78.6	10.5	1.54×10^5	7.2×10^{-15}	2.2×10^{-14}	5.2×10^{-14}	8.0×10^{-14}	1.0×10^{-13}	32.9
79.2	10.8	1.54×10^5	8.4×10^{-15}	3.4×10^{-14}	7.9×10^{-14}	1.5×10^{-13}	1.9×10^{-13}	34.9
79.2	10.8	1.54×10^5	3.0×10^{-14}	6.0×10^{-14}	1.0×10^{-13}	2.0×10^{-13}	3.3×10^{-13}	33.2
79.2	10.8	1.54×10^5	1.8×10^{-14}	4.2×10^{-14}	8.3×10^{-14}	1.6×10^{-13}	2.3×10^{-13}	33.7
79.2	10.8	1.54×10^5	1.7×10^{-14}	4.2×10^{-14}	7.8×10^{-14}	1.4×10^{-13}	2.0×10^{-13}	32.2
79.2	10.8	1.54×10^5	2.6×10^{-14}	9.0×10^{-14}	1.6×10^{-13}	2.6×10^{-13}	3.8×10^{-13}	33.9
79.2	10.8	1.54×10^5	1.5×10^{-14}	8.3×10^{-14}	1.7×10^{-13}	2.4×10^{-13}	3.1×10^{-13}	32.2
79.2	10.8	1.54×10^5	1.9×10^{-14}	7.6×10^{-14}	1.5×10^{-13}	2.3×10^{-13}	2.9×10^{-13}	30.7
79.2	10.8	1.54×10^5	2.8×10^{-14}	9.8×10^{-14}	1.8×10^{-13}	2.8×10^{-13}	3.4×10^{-13}	25.5
79.9	11.7	1.87×10^5	2.7×10^{-15}	8.1×10^{-15}	2.5×10^{-14}	5.5×10^{-14}	7.5×10^{-14}	46.2
79.9	11.7	1.87×10^5	2.3×10^{-15}	7.7×10^{-15}	2.6×10^{-14}	5.3×10^{-14}	7.0×10^{-14}	47.2
80.5	12.2	1.87×10^5	2.9×10^{-15}	8.8×10^{-15}	2.7×10^{-14}	5.8×10^{-14}	8.0×10^{-14}	44.7
82.6	14.0	6.56×10^5	2.8×10^{-15}	9.0×10^{-15}	3.1×10^{-14}	8.0×10^{-14}	1.1×10^{-13}	49.5
83.5	15.0	6.56×10^5	1.6×10^{-15}	8.8×10^{-15}	4.2×10^{-14}	1.1×10^{-13}	1.5×10^{-13}	57.2
83.5	15.0	6.56×10^5	2.2×10^{-15}	7.6×10^{-15}	3.0×10^{-14}	7.1×10^{-14}	9.7×10^{-14}	53.2
84.9	16.1	1.54×10^5	3.5×10^{-15}	1.3×10^{-14}	4.0×10^{-14}	9.3×10^{-14}	1.3×10^{-13}	49.0
84.9	16.1	1.54×10^5	2.7×10^{-15}	9.7×10^{-15}	3.4×10^{-14}	8.7×10^{-14}	1.3×10^{-13}	52.0

ACKNOWLEDGMENTS

This work was performed under Contract AT-11-1-GEN-14. The authors are grateful to the U.S. Atomic Energy Commission and to the Westinghouse Electric Corporation for permission to publish this work.

The authors sincerely appreciate the help of the personnel in the Ceramic Fuel Materials, Radiochemistry, and Metallography Groups. Particular acknowledgment is made to Dr. B. Lustman for initiating this study, to K. R. Bauer for assistance in carrying out the experimental measurements, to A. P. Hemphill for aid in the machine computations, and to Drs. J. Belle and J. M. Markowitz for their helpful discussion and criticism of this work.

REFERENCES

1. B. Lustman, "Irradiation Effects in Uranium Dioxide" in "Uranium Dioxide: Properties and Nuclear Applications," J. Belle, ed., pp. 431-666, U.S. Government Printing Office, Washington, D.C., 1961.

2. O. Hahn, "Applied Radiochemistry," Cornell University Press, Ithaca, New York, 1936.

3. S. Flugge and K. E. Zimens, "Determination of Grain Size and Diffusion Constant from the Emanation Power. Theory of the Emanation Method," Z. physik. Chem. B42, 179-220 (1939).

4. K. E. Zimens, "Surface Determination and Diffusion Measurements by Radioactive Noble Gases. (Practice and Quantitative Method.) I. The Practical Procedure of Measuring," Z. physik. Chem. A191, 1-53 (1942).

   K. E. Zimens, "Surface Determination and Diffusion Measurements by Radioactive Noble Gases. (Practice and Quantitative Method.) II. The Valuation of Data," Z. physik. Chem. A191.95-128 (1942).

   K. E. Zimens, "Surface Determinations and Diffusion Measurements by Means of Radioactive Inert Gases. III. The Process of Emission of the Radiation from Disperse Systems. Conclusions about the Evaluation of Emanating-Power Measurements and about the Interpretation of the Results," Z. physik. Chem. 192, 1-55 (1943).

5. A. C. Wahl and N. A. Bonner, Eds., "Radioactivity Applied to Chemistry," pp. 284-310, John Wiley & Sons, Inc., New York, 1951.

6. W. Jost, "Diffusion in Solids, Liquids, Gases," Rev. Ed., pp. 314-323, Academic Press, Inc., New York, 1960.

7. J. N. Gregory, "The Measurement of Emanating Power Using Thoron Gas in a Continuous Flow System," AERE-C/R-460, March 1950.

8. A. C. Wahl and W. R. Daniels, "Emanating Power of Barium Stearate for 3.9-Second Actinon (Radon-219)," J. Inorg. Nucl. Chem. 6, 278-287 (1958).

9. S. Aronson, J. C. Clayton, J. E. Rulli, and T. R. Padden, "Surface Areas of Sintered UO_2 Compacts," in "Bettis Technical Review, Reactor Technology," WAPD-BT-19, June 1960, pp. 83-92.

10. T. R. Padden, "Microscopy of Uranium Dioxide," in "Uranium Dioxide: Properties and Nuclear Applications," J. Belle, Ed., pp. 671-704, U.S. Government Printing Office, Washington D.C., (1961).

11. J. N. Gregory and J. Howlett, "A Mathematical Analysis of the Continuous Flow System for Measurement of Thoron Emanating Power," AERE-C/R-490, December 1950.

12. D. J. M. Bevan, "A New Experimental Factor Limiting the Quantitative Application of Emanating Power Measurements to the Study of Diffusion Problems," AERE-C/R-988, July 16, 1952.

13. J. S. Anderson, E. A. Harper, S. Moorbath, and L. E. J. Roberts, "The Properties and Microstructure of Uranium Dioxide; Their Dependence upon the Mode of Preparation," AERE-C/R-886, August 19, 1952.

14. J. S. Anderson, "Developments in the Hahn Emanation Technique," Proc. Intern. Symposium Reactivity of Solids, Gothenburg 1952, Pt. 1, 37-40 (Pub. 1954) (in English).

15. J. S. Anderson, D. J. M. Bevan, and J. P. Burden, "The Behaviour of Recoil Atoms in Ionic Solids," Proc. Roy. Soc. (London) 272A, 15-32 (1963).

16. L. G. Cook, "Investigations on Chromium and Iron Hydroxides and Their Significance for the Emanation Method," Z. physik. Chem. B42, 221-239 (1939).

17. R. Jagitsch, "Investigations of Spontaneous Diffusion and Chemical Transformation in Solid Substances by use of Emanation as an Indicator," Trans. Chalmers Univ. Technol., Gothenburg, Sweden No. 11, 3-47 (1942).

18. J. N. Gregory and S. Moorbath, "The Diffusion of Thoron in Solids, Part I. Investigations on Hydrated and Anhydrous Alumina at Elevated Temperatures by Means of the Hahn Emanation Technique," Trans. Faraday Soc. 47, 844-859 (1951).

19. L. E. J. Roberts, "Uranium Dioxide as a Fuel Element," AERE-C/M-268, January 23, 1956.

20. R. Lindner and H. J. Matzke,"Diffusion of Radon in Oxides after Recoil Doping," Z. Naturforsch. 15a, 1082-1086 (1960). Translated by Gordon R. Love and Published as AEC-tr-5058.

21. H. J. Matzke and R. Lindner, "Diffusion of Xe^{133}, Rn^{222} and I^{131} in ThO_2," Z. Naturforsch. 15a, 647-648 (1960).

22. R. Lindner, H. Matzke, and F.Schmitz, "Fission Product Diffusion and Self Diffusion in High Temperature Nuclear Fuels," Z. Elektrochem. 64, 1042-1045 (1960). Translated by Gordon R. Love and Published as AEC-tr-5206.

23. A. H. Booth and G. T. Rymer, "Determination of the Diffusion Constant of Fission Xenon in UO_2 Crystals and Sintered Compacts," CRDC-720, August,1958.

24. R. Lindner and H. Matzke, "Diffusion of Xenon-133 from Uranium Oxides," Z. Naturforsch. 13a, 794-796 (1958).

25. R. Lindner and H. J. Matzke, "Diffusion of Xenon-133 in Uranium Oxides Having Different Oxide Contents," Z. Naturforsch. 14a, 582-584 (1959).

26. W. H. Stevens, J. R. MacEwan, and A. M. Ross, "The Diffusion Behavior of Fission Xenon in Uranium Dioxide" in "Nuclear Reactor Chemistry. First Conference, Gatlinburg, Tennessee, October 12-14, 1960," TID-7610, pp. 7-22.

27. H. J. Matzke and R. Lindner, "The Diffusion of Homogeneously Distributed Noble Gases from Solids," Z. Naturforsch. 16a, 845-849 (1961).

28. R. Lindner and H. Matzke, "Diffusion of Radioactive Noble Gases in Uranium Oxides and Uranium Monocarbide," Z. Naturforsch. 14a, 1074-1077 (1959).

29. A. B. Auskern, "The Diffusion of Krypton-85 from Uranium Dioxide Powder," WAPD-TM-185, February, 1960.

30. J. Belle, A. B. Auskern, W. A. Bostrom, and F. S. Susko, "Diffusion Kinetics in Uranium Dioxide" in "Reactivity of Solids," J. H. de Boer, et al, Eds., pp. 452-446, Elsevier Publishing Company, Amsterdam, 1960.

31. A. B. Auskern, "Further Work on the Diffusion of Krypton-85 from Uranium Dioxide Powder," WAPD-TM-225, August, 1960.

32. W. B. Cottrell, H. N. Culver, J. L. Scott, and M. M. Yarosh, "Fission-Product Release from UO_2," ORNL-2935, September 13, 1960.

33. A. V. Pace, "CURF 1-A Least-Squares Polynominal Fitting Program for the Philco-2000," WAPD-TM-226, January, 1961.

34. "Minutes of the French-Canadian Discussion on the Behaviour of Fission Gases in Uranium Oxide, September 26-27, 1961." France. Commissariat a l'Energia Atomique. Centre d'Etudes Nucleaires, Saclay. Translated by A. L. Monks, January 29, 1962, and Published as AEC-tr-5103.

35. J. Belle, "Properties of Uranium Dioxide" in "Proceedings of the Second United Nations International Conference on the Peaceful Uses of Atomic Energy, Geneva, 1958," Vol. 6, p. 585, United Nations, Geneva, 1958.

36. W. E. Garner, Ed., "Chemistry of the Solid State," p. 307 Academic Press, Inc., New York, 1955.

37. G. W. Parker, G. E. Creek, and W. J. Martin, "Fission Product Release from UO_2 by High Temperature Diffusion and Melting in Helium and Air," CF-60-12-14, February 14, 1961.

38. R. H. Barnes, M. Kangilaski, J. B. Melehan, and F. A. Rough, "Xenon Diffusion in Single-Crystal and Sintered UO_2," BMI-1533, August 1, 1961.

39. J. A. L. Robertson, "Concerning the Effects of Excess Oxygen in UO_2." CRFD-973, October, 1960.

40. W. B. Lewis, "Behavior of Fission Gases in UO_2 Fuel," DL-45, November, 1961.

41. J. B. Melehan, R. H. Barnes, J. E. Gates, and F. A. Rough, "Release of Fission Gases from UO_2 during and after Irradiation," BMI-1623, March 26, 1963.